The Role of Microstructure on the Strength and Toughness of Fully Pearlitic Steels

J. M. HYZAK AND I. M. BERNSTEIN

An experimental program was carried out to clarify the structure-property relationships in fully-pearlitic steels of moderately high strength levels, and to identify the critical microstructural features that control the deformation and fracture processes. Specifically, the yield strength was shown to be controlled primarily by the interlamellar pearlite spacing, which itself was a function of the isothermal transformation temperature and to a limited degree the prior-austenite grain size. Charpy tests on standard and fatigue precracked samples revealed that variations in the impact energy and dynamic fracture toughness were dependent primarily on the prior-austenite grain size, increasing with decreasing grain size, and to a lesser extent with decreasing pearlite colony size. These trends were substantiated by a statistical analysis of the data, that identified the relative contribution of each of the dependent variables on the value of the independent variable of interest. The results were examined in terms of the deformation behavior being controlled by the interaction of slip dislocations with the ferrite-cementite interface, and the fracture behavior being controlled by a structural subunit of constant ferrite orientation. Preliminary data suggests that the size of such units are controlled by, but are not identical to, the prior-austenite grain size. Possible origins of this fracture unit are considered.

THE relation of microstructure to mechanical properties in carbon steels has been the subject of considerable research. It is well known for example that increasing the carbon content increases a steel's strength, but usually only at the expense of fracture toughness. More specifically, however, there is considerable debate as to how microstructural variations affect mechanical properties. We intend to examine the origin of such variations for fully pearlitic eutectoid steels.

It is generally agreed that in high carbon near-eutectoid steels, it is the pearlite rather than proeutectoid ferrite that controls strength, and refining the pearlite interlamellar spacing results in an increase in yield strength.[1-3] However, the fracture process in pearlitic steels is less well understood. This is due, in part, to the difficulty in isolating different microstructural variables. There have been conflicting results reported in the literature as to the effects of pearlite interlamellar spacing,[4,5] pearlite colony size,[1] and prior-austenitic grain size[6] on the toughness of steel. Differences in carbon level, alloy content, and processing conditions among the steels examined make definitive evaluation of the literature results difficult.

The present work was undertaken, therefore, to clarify the structure-property relationships in fully-pearlitic steel, and to identify which of the above critical microstructural features control the deformation and fracture processes.

EXPERIMENTAL

Material

The material used for this investigation was supplied by the Association of American Railroads as hot rolled rail steel stock. The chemical composition was analyzed to be: C-0.81 wt pct, Mn-0.87 wt pct, P-0.018 wt pct, S-0.013 wt pct, Si-0.17 wt pct and Fe-Balance.

Both standard ASTM Charpy and tensile blanks were cut from the stock so that the fracture plane of each specimen would be transverse to the rolling direction.

Heat Treatment

Specimens were heat treated over a range of temperatures for various times to produce a systematic variation in microstructure (Table I). Oversized blanks (12 mm sq.), were austenitized for 1 to 3 h in the temperature range from 1073 K (1472°F) to 1473 K (2192°F). The finest grain structure was developed by rapidly austenitizing the samples to a temperature of approximately 1103 K (1526°F), and subsequently

Table I. Heat Treatment Schedule for Eutectoid Steel

Heat Treatment	Austenization* Temperature K	Austenization* Temperature °F	Salt Bath Temperature K	Salt Bath Temperature °F
1†	1103	(1526)	838	(1049)
2†	1103	(1526)	858	(1085)
3†	1103	(1526)	898	(1157)
4†	1073	(1472)	823	(1072)
5	1073	(1472)	838	(1049)
6	1073	(1472)	858	(1085)
7	1073	(1472)	898	(1157)
8	1073	(1472)	948	(1247)
9	1143	(1598)	823	(1022)
10	1143	(1598)	838	(1049)
11	1143	(1598)	858	(1085)
12	1143	(1598)	898	(1157)
13	1273	(1832)	823	(1022)
14	1273	(1832)	858	(1085)
15	1473	(2192)	858	(1085)
16‡	1473	(2192)	858	(1085)
17	As Received Rail Structure			

*Austenization time—1 h.
†Thermal cycle treatment.
‡Austenization time—3 h.

J. M. HYZAK is Metallurgist, Air Force Materials Laboratory, (LLN), Wright Patterson Air Force Base, Dayton, OH 45433. I. M. BERNSTEIN is Associate Professor, Department of Metallurgy and Materials Science, Carnegie-Mellon University, Pittsburgh, PA 15213.

Manuscript submitted September 23, 1975.

transforming below the A_1 before there was time for substantial grain growth in the high temperature range.[7] After austenitizing, specimens were transformed to pearlite in salt pots held at various temperatures in the range 823 K (1022°F) to 948 K (1247°F). Transformation times were chosen sufficient to ensure complete transformations, without appreciable spheroidization. Specimens were then machined to final size; for the Charpy this was 10 mm sq, and for the tensiles this was to a gage diam of 6.35 mm. Although the actual transformation temperature was higher than the salt bath temperature (by as much as 40°C for the lowest temperature), the transformation was sensibly isothermal in nature. This was confirmed by pearlite spacing and hardness measurements taken on cross-sections of specimens machined to final size. Inasmuch as reaction kinetics were not of interest in this study, the transformation will be described by the bath rather than the reaction temperature.

Quantitative Metallographic Techniques

Quantitative analyses of the microstructure developed from each of the heat treatments included measurements of the prior-austenite grain diameter, the pearlite colony diameter, and the pearlite interlamellar spacing.

The random intercept method[8] was used to determine the austenite grain size. Measurements were taken from coupons that had been austenitized with the test specimens, quenched, and subsequently heat treated and etched to reveal the grain structure. Tempering these coupons at 783 K (950°F) for 16 h, followed by etching in boiling picric acid, successfully revealed the prior-austenite structure as dark grain boundaries on a white matrix.[7]

In order to better resolve the pearlite structure, electron transmission microscopy employing conventional two-stage carbon replica techniques was used. The colony size was determined from the same micrographs by the random intercept method.

After considerable preliminary study, it was decided to obtain the pearlite spacing by measuring the interlamellar distance in those colonies where the plates were oriented nearly perpendicular to the plane of observation. The pearlite in these colonies would thus be most likely to project the true spacing. This method was chosen in order to reduce the statistical counts needed, especially when using the random intercept technique. Measurements were made along secants drawn perpendicular to these colonies in similar fashion to the work of Brown and Ridley.[9] Results of this technique compared favorably with limited data obtained using the random intercept method, and, as mentioned, were not a function of location in the cross-section.

Mechanical Testing

The testing program included both tensile and instrumented impact tests. Room temperature tensile tests were performed at a strain rate of 0.01 per min. Both the yield strength (0.2 pct offset) and the reduction in area were calculated and correlated with microstructure variations due to heat treatment.

Dynamic instrumented impact tests, on precracked Charpy specimens, were chosen to evaluate the impact fracture toughness as a function of heat treatment.[10] An instrumented impact system utilizes strain gages mounted in the striking tup to sense and record the load-time history of the fracture process. In addition, the more conventional measure of toughness, energy absorbed, is also recorded. From these data, both W/A (absorbed energy per fractured area) and dynamic fracture toughness, K_{ID}, values were determined for each test condition.

K_{ID} is the fracture toughness of a material as measured under dynamic or impact conditions. For these experiments the stress intensity rate, ($\dot{K}$), was 3.3 to 4.4 $\times 10^5 \frac{N}{m^{3/2}\,s}$. Since there is as yet no standardized procedure for this type of testing and data reduction, calculation of K_{ID} values from test data is discussed in Appendix 1, for both the elastic and plastic types of fracture. While the physical significance of K_{ID} values may be a source of disagreement due to nonstandardized test methods, they are none the less important as an additional means of evaluating relative changes in impact toughness levels. It should be noted that changes in dynamic fracture toughness correlated well with variations in impact energy for this series of experiments.

The results of the impact toughness tests will be represented primarily as Charpy transition curves, and only the Charpy transition will be correlated with microstructure. The Charpy transition temperature reported herein will be the temperature corresponding to a W/A ratio of 13.5 $\times 10^4 \frac{N}{m}$ (71 ft lb/in.^{2}). This value is roughly equal to one-half the difference between the lower and upper shelf energy, a value frequently used in the past as a measure of transition temperature.[11]

Statistical Analysis

Multiple-linear regression analyses were performed to determine statistically the dependence of the variables, yield strength, Charpy transition temperature, and reduction in area, on the three microstructural parameters of interest, *viz*, austenite grain size, pearlite colony size, and pearlite interlamellar spacing. A basic linear multiple regression computer subprogram was used. Because the program did not have the capability of determining the functional dependence of each dependent variable, the functional relationships had to be assumed. The final analysis was based on the relationships of $d^{-1/2}$ (grain size$^{-1/2}$), $P^{-1/2}$ (colony size$^{-1/2}$), and $S^{-1/2}$ (pearlite spacing$^{-1/2}$). In preliminary analyses, these relationships gave the best correlation with the experimental data. Functional relationships of this type have been previously described in the literature[1-3] for similar types of steels. A complete description of the analyses is contained in Appendix 2. The units for the three structural parameters, grain and colony size and pearlite spacing are in centimeters.

EXPERIMENTAL RESULTS

Microstructure

Results of the quantitative microscopy aspect of the study are presented in Table II. Examination of the microstructure for each heat treatment revealed a

Table II. The Effect of Heat Treatment on Microstructure of Eutectoid Steel

Heat Treatment	Austenitic Grain Size, 10^{-3} cm	Pearlite Colony Size, 10^{-4} cm	Pearlite Spacing, 10^{-6} cm
1	1.43	4.78	14.10
2	1.43	4.57	15.35
3	1.43	5.26	19.50
4	2.52	5.38	13.00
5	2.52	4.75	13.75
6	2.52	6.58	15.16
7	2.52	6.09	17.50
8	2.52	6.34	27.00
9	3.51	6.04	12.10
10	3.51	5.33	14.00
11	3.51	4.29	14.10
12	3.51	5.15	16.35
13	4.02	5.56	11.93
14	4.02	5.76	13.75
15	14.73	5.67	13.62
16	16.65	5.70	11.57
17	13.0*	7.12	15.67

*Estimated.

(The uncertainty in the values for grain size, colony size and pearlite spacing is of the order of 10 pct.)

Table III. Effect of Heat Treatment on Mechanical Properties of Eutectoid Steel

Heat Treatment	Charpy Transition Temperature, °F: K	Charpy Transition Temperature, °F: °F	Yield Strength, ksi: (MN/m²)	Yield Strength, ksi: ksi	Reduction in Area, Pct	Hardness, R_c
1	397	220	544.0	78.9	47.9	23.7
2	369	205	509.5	73.9	44.5	22.8
3	369	205	437.1	63.4	43.5	16.0
4	395	252	570.2	82.7	32.1	27.7
5	390	243	568.8	82.5	33.2	27.3
6	397	255	546.1	79.2	28.8	26.3
7	405	270	479.9	69.6	22.5	22.1
8	400	260	422.0	61.2	26.8	17.3
9	402	265	633.6	91.9	36.1	28.6
10	405	270	580.5	84.2	30.0	28.3
11	401	263	559.9	81.2	29.9	26.1
12	405	270	467.5	67.8	24.5	21.7
13	406	272	621.2	90.1	32.5	30.8
14	402	265	610.9	88.6	31.0	29.0
15	433	320	620.5	90.0	15.2	28.8
16	433	420	620.5	90.0	9.6	30.6
17	430	315	505.4	73.3	14.0	24.0

fully pearlitic structure. As expected, austenite grain size increased with increasing austenization time and temperature, from 1.43×10^{-3} cm to 16.65×10^{-3} cm. As noted previously, the finest austenite grain structure was produced by a rapid thermal cycle technique.[7]

The pearlite interlamellar spacing was a strong function of the isothermal transformation temperature; the pearlite spacing also increased as the prior austenite grain diameter decreased. This rather interesting result, substantiated by statistical analysis (see Appendix **2.13**), has also been observed by Gladman *et al*[1] in a recent paper on continuously cooled steels, and by others.[12] The reason for this behavior is not clear, but it does not appear to be related to variations in austenitizing temperature and subsequent changes in cooling rate. To demonstrate this, specimens step-quenched from a higher austenitizing temperature (*e.g.*, 1273 K) to a lower one (*e.g.*, 1073 K) had a finer pearlite spacing than specimens austenitized only at 1073 K. This is an intriguing result which clearly deserves further study.

For the heat treatments performed, the pearlite colony diameter was relatively constant, in the range 4.5 to 6.0×10^{-4} cm. Gladman[1] has reported a much larger range of colony size than reported herein, for steels continuously cooled, but of variable composition. Because of the small variation in colony size in this study, it will be difficult to determine conclusively to what extent pearlite colony structure affects mechanical properties. The large variations in properties that are observed however, tends to negate any critical role of colony size in controlling resultant properties.

Strength and Hardness

As expected, both the room temperature yield stress and hardness were found to be a strong function of the pearlite interlamellar spacing. For a given prior austenitic grain size, there is typically a 20 to 30 pct increase in the 0.2 pct offset yield stress going from the coarsest pearlite spacing developed in this program to the finest (Table III). A larger pearlite range was not studied because of our interest in this steel's behavior at high strength levels.

The regression equation found to best describe the relationship between yield stress and the three microstructural features is:

$$\sigma_{ys}\,(\text{Ksi})^* = 3.16 \times 10^{-1}\,(S^{-1/2}) - 5.79 \times 10^{-2}\,(P^{-1/2}) - 4.17 \times 10^{-1}\,(d^{-1/2}),\ +\ 7.58,$$

*1 ksi = 6.89 MPa. $K = (5/9)(°F + 459.67)$.

with standard errors of the coefficients of 4.61×10^{-2}, 4.19×10^{-1} and 2.25×10^{-1}, respectively. According to the statistical treatment, comparison of the standard error of the coefficient to its corresponding regression coefficient gives a measure of the correlation between variables. A relatively large error would indicate that the two variables are not significantly related. The computed T value which is simply the regression coefficient divided by the standard error of the coefficient is presented in Appendix 2 for the purpose of comparison; the greater the absolute value of T the better the correlation between variables.

Thus, the previous equation shows that increases in yield strength correlate best with decreases in pearlite spacing, and although the prior austenite grain size also has an effect on strength, the correlation is not as great. Indeed, further analyses (Appendix **2.8, 2.9, 2.10**) indicate that pearlite spacing alone can account for 84 pct of the variation in strength, while grain size can only account for 37 pct. Variations in pearlite colony size have minimal effect on strength for the limited range available in this study, as shown by the standard error of the coefficient being larger than the regression coefficient.

The analyses indicate that yield stress does increase somewhat as prior austenite grain size increases. However, this is probably not a direct effect of grain size on the deformation process, but instead is attributable to the relationship between grain size

and pearlite spacing. As mentioned above, for a given isothermal transformation temperature, pearlite spacing decreases as the grain size increases. Therefore, the beneficial effect of a large grain size on strength is not a direct effect, but results from a refinement of the pearlite spacing.

The complete range of data is summarized in Fig. 1. The graph bears out the conclusion that strength is primarily a function of the pearlite interlamellar spacing, and also that the relationship is satisfactorily represented by an inverse squared power law.

Toughness

Impact toughness, as measured by the Charpy transition temperature, ranged from 205°F (368 K) for two fine-grained microstructures to 315°F (430 K) for the coarsest grained steel (Table III). The best fit regression equation, containing terms for each of the three microstructural variables was determined to be: $\text{T.T.}\,(°\text{F}) = -8.25 \times 10^{-2}\,(S^{-1/2}) - 1.22\,(P^{-1/2}) - 5.55\,(d^{-1/2}) + 4.35 \times 10^{2}$ with standard errors of the coefficients of 8.74×10^{-2}, 7.94×10^{-1} and 4.27×10^{-1}, respectively.

The large standard error of the coefficient for the pearlite spacing factor indicates that there is no significant correlation between toughness and pearlite spacing. Prior-austenite grain size, however, correlated well with transition temperature. In fact in a separate analysis (Appendix **2.3**), grain size was able to account for 94 pct of the variation in toughness. The statistical fit is increased at the 10 pct significance level by retaining the term for pearlite colony size, suggesting that this factor can contribute.

The resultant regression equation incorporating only these two terms is: $\text{T.T.}\,(°\text{F}) - 1.49\,(P^{-1/2}) - 5.33\,(d^{-1/2}) + 4.21 \times 10^{2}$ with standard errors of the coefficients of 7.49×10^{-1} and 3.57×10^{-1}, respectively. Note that the prior austenite grain term has a regression coefficient larger than that for colony size by a factor of approximately 4 to 1. This supports the graphical results, plotted in Fig. 2, and indicates that grain size is the effective means of influencing the toughness of eutectoid steel.

Fig. 2 shows that the Charpy transition temperature is shifted down the temperature scale as the grain size is decreased, with the pearlite spacing maintained at a constant value. The conjugate case is represented in Fig. 3; here the prior-austenitic grain size is kept constant and the pearlite spacing is varied, with no apparent effect on the transition temperature. The complete range of data is summarized in Fig. 4 by plotting Charpy transition temperature *vs* $(d^{-1/2})$. These data support the previous conclusion that toughness is primarily a function of prior-austenite grain size.

The corresponding values of dynamic fracture toughness, (K_{ID}), associated with the data of Fig. 2 are illustrated in Fig. 5. At a temperature of 0°F, the dynamic fracture toughness, K_{ID}, increased from approximately 20 ksi $\sqrt{\text{in.}}$ (22 MN/m$^{3/2}$) to 38 ksi $\sqrt{\text{in.}}$ (41.7 MN/m$^{3/2}$) by refining the grain size an order of

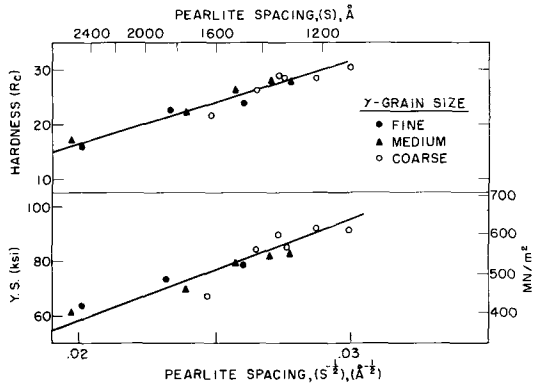

Fig. 1—Yield strength and hardness *vs* pearlite interlamellar spacing.

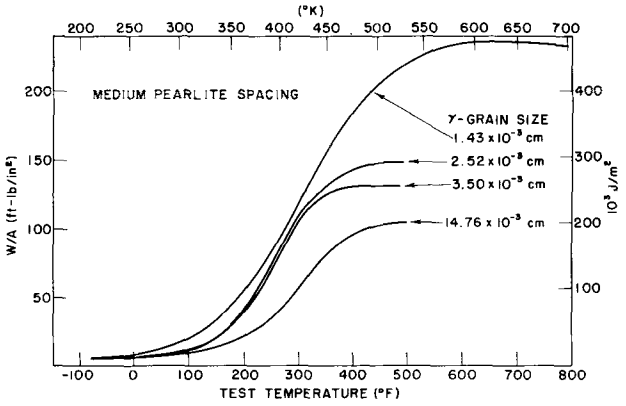

Fig. 2—Charpy transition curves as a function of prior austenitic grain size.

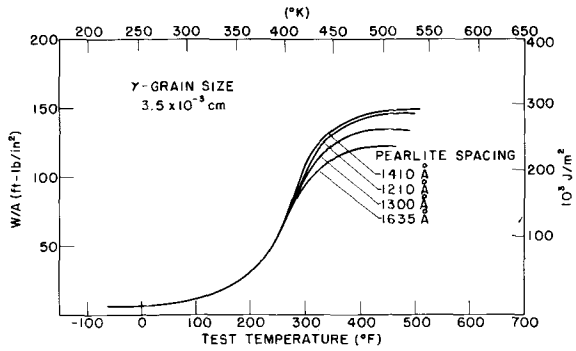

Fig. 3—Charpy transition curves as a function of pearlite interlamellar spacing.

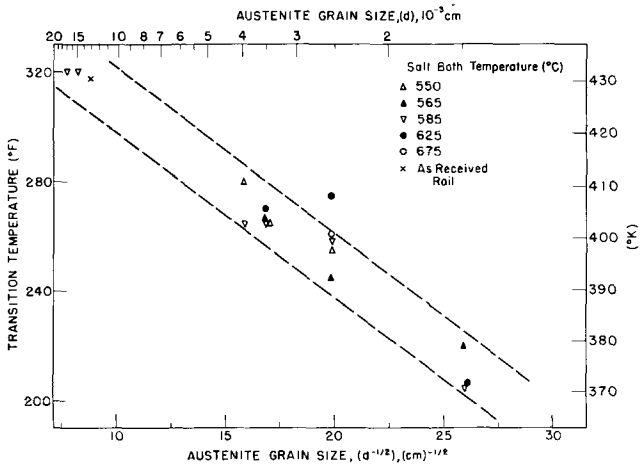

Fig. 4—Charpy transition temperature *vs* prior austenitic grain size.

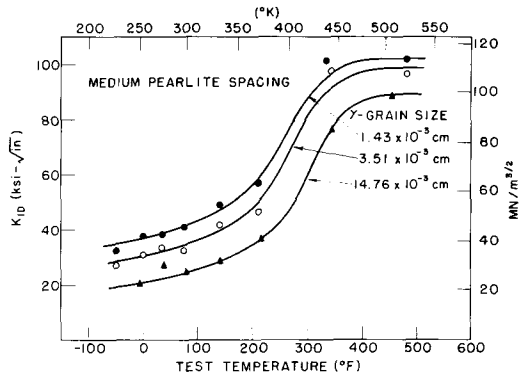

Fig. 5—Dynamic fracture toughness, K_{ID}, curves as a function of prior austenitic grain size.

magnitude. This corresponds to an increase in critical flaw size of almost a factor of four. The above illustration shows that for dynamic service application, microstructural manipulations can affect a large change in the critical crack size, putting it for some loading situations into the detectable size range for nondestructive testing.

Finally, it is of interest to examine the role of microstructure on the upper shelf energy (Figs. 2 and 3). A refined austenite grain size greatly increases the energy absorbed during the plastic tearing processes normally associated with the upper shelf. The pearlite spacing has a nonsystematic effect; if anything, the upper shelf energy shows a tendency to increase with decreasing pearlite spacing. It seems clear that for eutectoid steels, the critical structural parameter controlling toughness is the austenite grain size. This behavior extends to the case of tensile ductility as discussed in the next section.

Ductility

Ductility, as measured by the reduction in area, varied with microstructure from approximately 10 pct to 50 pct. The regression equation correlating reduction in area to microstructure was: R_A (pct) = $1.24 \times 10^{-1} (S^{-1/2}) + 2.66 \times 10^{-1} (P^{-1/2}) + 1.85 (d^{-1/2}) - 4.71 \times 10^{1}$ with standard errors of the coefficients of 4.95×10^{-2}, 4.50×10^{-1} and 2.42×10^{-1}, respectively.

Examination of the regression coefficients indicates that the prior austenite grain diameter has the greatest influence on ductility, with pearlite spacing having a more modest effect and colony size (for the range available in this study) having little effect.

DISCUSSION

It has been shown that the strength of fully pearlitic eutectoid steel is controlled microstructurally by the pearlite interlamellar spacing, while fracture toughness and tensile ductility vary inversely with prior austenitic grain size. The results also suggest, based on a limited range of data, that pearlite colony size does not significantly affect strength, and has, at most, a secondary influence on toughness. A major significance of these results is that strength and toughness are controlled by different microstructural parameters, and thus, an increase in either property need not be compromised, as in the more common case when the two properties are inversely related.

The dependence of the yield strength of high carbon steels on pearlite spacing has been previously reported in the literature.[1,3] These studies concluded that the flow stress of pearlite follows a Hall-Petch relationship:

$$\sigma_y = \sigma_i + k_y (S)^{-1/2}$$

which also fits the data reported herein. Karlsson *et al*[13] have recently summarized existing data for eutectoid steels and have stated that a best mean value of the Hall-Petch slope (k_y) for the yield stress is 0.25 MN/m$^{3/2}$ which is in excellent agreement with the value of 0.246 MN/m$^{3/2}$ obtained in this study. It should be noted that the regression analysis for the results of this study resulted in a negative intercept which although clearly inconsistent with the definition of friction stress as the stress for dislocation movement in the lattice, has also been reported in two of the three studies on eutectoid steel.[2,3] A statistically satisfactory correlation can also be obtained with S^{-1}, and a positive friction stress is obtained. The lack of a rigorous model for either function makes further analysis unnecessary. The Petch slope value obtained from the former relationship is in good agreement with a variety of iron alloys, implying that carbide-ferrite interfaces and ferrite-ferrite interfaces are equally effective dislocation barriers.

The explanation generally advanced as to why the flow strength should be controlled by the pearlite spacing is that the available slip distance, in this case the distance between pearlite lamellae, is the most important variable in determining strength. This explanation is quite reasonable since it has been shown that carbide lamellae are effective barriers to dislocation motion.[14] In fact, this argument is essential to several theories of microcrack initiation in pearlite which require the stress buildup at the carbide-ferrite interface to be large enough to cleave the carbide lamella.[15]

The fracture process in eutectoid steels, however, is less well understood. Austenitic grain size,[6] pearlite colony size,[1] and pearlite spacing[4,5] have all previously been correlated with toughness in the literature. The present research has demonstrated that varying the prior-austenitic grain size has a much greater effect on the subsequent fracture toughness than varying the pearlite spacing or colony size.

The effect of pearlite interlamellar spacing on toughness has been a matter of controversy in the literature. We believe that this uncertainty may be due, in part, to the varied carbon and alloy contents of the previously studied steels, since the present data indicates little or no effect of pearlite spacing on impact fracture toughness of precracked specimens. An explanation proposed by Gladman *et al*, who found similar results using *V*-notch specimens, is that the effect of cementite plate thickness and ferrite spacing tend to cancel one another out, with the advantages of a reduction in cementite plate thickness being offset by the harmful effects of refining the interlamellar ferrite spacing. Although this rationalization accounts for the data, we believe it more likely that running cleavage cracks are for all practical purposes insensitive to interpearlite structure, so long as the pearlitic ferrite orientation is continuous. We shall return to this point.

It may also be worthwhile to mention that in preliminary testing using unprecracked V-notch specimens, the V-notch transition temperature was affected to a greater extent by variations in pearlite spacing than was the value obtained with dynamic fracture toughness specimens. This would indicate that the initiation process in these steels is more sensitive to pearlite structure than the propagation phase, a result consistent with cracks being initiated at stress concentrations at the ferrite-carbide interface.

The remaining parameter that has not been considered, and that can be controlled by the prior-austenitic grain size, is the relative crystallographic orientations of the various microstructural units. Previous researchers[6,16] who have studied the fracture process in pearlitic steels, have noted that the cleavage cracks apparently follow certain cleavage planes in the ferrite laths. Thus, if the prior-austenite grain structure can control the resultant ferrite orientations in pearlite, it may explain the influence of grain size on toughness.

To model the situation, consider that toughness is related to the number of mismatch boundaries in a microstructure at which a running crystallographic cleavage crack must alter direction, possibly by renucleation or by some other energy absorbing process. For pearlitic steels, Turkalo[6] has observed that the fracture path often continued as a single cleavage facet across a number of pearlitic colonies, extending over part of, or in some cases, the whole of one former austenite grain. This would seem to imply that the ferrite from a single austenite grain has a preferred orientation, such that cleavage planes in adjacent pearlite colonies are continuous or closely aligned. In line with this thinking, a finer prior austenitic grain size would lead to smaller units of preferred ferrite orientation and, therefore, a higher fracture toughness.

An alternative explanation, based on Smith's[17] results on pearlite growth in eutectoid steel is that for a given transformed austenite grain, the ferrite laths in pearlite should bear a specific orientation relationship to a neighboring grain of austenite; this adjacent grain being the true parent grain for the crystal of ferrite. This, of course, differs from the explanation proposed above, which required the pearlitic ferrite of each colony be related to the prior-austenite grain in which it is contained. In this model, the effect of prior-austenite grain size on toughness is explainable by relating austenite grain diameter to the number and size of orientation "units" in the pearlite. Each "unit" is made up of adjacent pearlite colonies of common parentage and therefore common ferrite orientation. In a structure that has a large prior-austenitic grain size, there may be several colonies nucleated on a given grain side and therefore of the same 'unit' parentage. In a fine grained structure far fewer colonies would have common parentage, so each "unit" may be comprised of as few as one colony. For an equal pearlite colony size, the fine-grained structure would thus have considerably more orientation "units" and, therefore, would present more resistance to crack propagation. In support of this approach, Dippenaar and Honeycombe[18] recently found, in a high manganese steel, that the pearlitic ferrite and cementite are related to the austenite grain into which they are not growing.

To ascertain which of the two proposed models is operative requires being able to differentiate between prior-austenite and colony boundaries in fully eutectoid steels, in order, for example, to show if there is a one-to-one correspondence between a fracture facet and a prior-austenite grain. Such studies are underway, as are orientation determinations of the ferrite within adjacent colonies. As part of this more comprehensive study, Park[19] has measured the facet size in more than one hundred fractured precracked Charpy specimens. He finds that while the average facet size is a strong function of the prior-austenitic grain size, it is always somewhat less, particularly for larger grain sizes. As expected from our results, he finds little systematic variation between pearlite spacing and facet size. The lack of direct correspondence between prior-austenitic grain size and facet size tends to support the approach of Smith[17] and Dippenaar and Honeycombe,[18] although considerably more work is needed to establish the origin of these pearlite colony units.

CONCLUSIONS

1) The strength and toughness of fully pearlitic steel are controlled by different microstructural parameters, and can be varied independently of one other to optimize service performance in such materials as rail steel.

2) Strength is dependent on the pearlite interlamellar spacing; decreasing the spacing results in an increase in strength. Pearlite spacing can be refined by decreasing the transformation temperature and to a lesser extent by increasing the austenitic grain size. The reason for this latter effect is not known.

3) Fracture toughness is more strongly a function of the prior-austenitic grain size. The finer the grain size, the greater the toughness. Pearlite colony size for the range studied has a minor influence at best on toughness. The fact that large variations in toughness are possible with little change in colony size, suggests that this is not a useful microstructural parameter to control toughness.

4) The results of this study suggest that the fracture process is controlled by a structural unit made up of a number of colonies, within which the ferrite should have the same crystallographic orientation. The size of this unit is controlled by, but is not identical to, the prior austenitic grain size.

APPENDIX 1

Dynamic fracture toughness values were calculated using instrumented impact data for both the linear elastic type of fracture, and the case of yielding before fracture. For the linear elastic case, a "valid" toughness value may be obtained for dynamic testing by applying linear elastic fracture mechanics, Ref. 1a:

$$K_{ID} = \frac{1.5\, Y\, L\, (P_F)\, a^{1/2}}{BW^2} \qquad \text{Eq. [1A]}$$

where

Y = function of (a/W)

L = support span width
P_F = load at fracture
a = total crack depth
B = thickness
W = width.

When the appropriate Charpy and load dimensions (in inches and pounds are considered), Eq. [1] reduces to:

$$K_{ID} = 38.7\ Y(P_F)\, a^{1/2}. \qquad \text{Eq. [2A]}$$

There is considerable controversy regarding the calculation of a meaningful fracture toughness value based on data derived from a specimen which fractures after general yielding. Several methods have been developed, however, for estimating the material's toughness, had the test sample been large enough for linear elastic fracture to occur. The lower-bound equivalent-energy approach was used for this study.[2a,3a] This method assumes that for a valid size specimen, fracture would have occurred at an energy equivalent to the initiation energy (energy at maximum load) measured for the Charpy size specimen. From this method, extrapolated values of P_F, corrected for machine compliance, are used in Eq. [2A] to obtain K_{ID}.[4a]

APPENDIX 2

Multiple linear regression analyses were performed in order to determine which microstructural parameters are related to each mechanical property, and, if possible, to rate the variables in order of their importance. As previously mentioned, the Computer Science Corporation (CSCX) commercial basic multiple linear regression analyses program was used. The results of each analyses are contained in this section.

For each analysis, the independent and dependent variables are identified as numbers. The data matrix contained the following parameters:

1	pearlite spacing	$S^{-1/2}$
2	pearlite colony size	$P^{-1/2}$
3	austenite grain size	$d^{-1/2}$
4	transformation temperature	(°C)
5	austenite grain size	d
6	Charpy transition temperature	(°F)
7	yield strength	(Ksi)
8	reduction in area	(pct)
9	hardness	(R_c)

The units for 1 to 3 have been given in the text.

2.1) Dependent Variable—6
Independent Variables—1, 2, 3

Variable	Regression Coefficient	Standard Error Coefficient	Computed T
1	− 8.25 E−02	8.74 E−02	− 9.44 E−01
2	− 1.22 E+00	7.94 E−01	− 1.54 E+00
3	− 5.55 E+00	4.27 E−01	− 1.29 E+01

R-squared = 0.957 (gives the confidence to which the dependent variable can be accounted for in terms of the independent variables).

2.2) Dependent Variable—6
Independent Variables—2, 3

Variable	Regression Coefficient	Standard Error Coefficient	Computed T
2	−1.49 E+00	7.43 E−01	−2.00 E+00
3	−5.33 E+00	3.57 E−01	−1.49 E+01

R-squared = 0.954.

2.3) Dependent Variable—6
Independent Variable—3

Variable	Regression Coefficient	Standard Error Coefficient	Computed T
3	−5.55 E+00	3.75 E−01	−1.48 E+01

R-squared = 0.939.

2.4) Dependent Variable—6
Independent Variable—2

Variable	Regression Coefficient	Standard Error Coefficient	Computed T
2	−4.85 E+00	2.90 E+00	−1.67 E+00

R-squared = 0.166.

2.5) Dependent Variable—6
Independent Variable—1

Variable	Regression Coefficient	Standard Error Coefficient	Computed T
1	4.49 E−01	3.02 E−01	1.49 E+00

R-squared = 0.136.

2.6) Dependent Variable—7
Independent Variables—1, 2, 3

Variable	Regression Coefficient	Standard Error Coefficient	Computed T
1	3.16 E−01	4.61 E−02	6.85 E+00
2	−5.79 E−02	4.19 E−01	−1.38 E−01
3	−4.17 E−01	2.25 E−01	−1.85 E+00

R-squared = 0.883.

2.7) Dependent Variable—7
Independent Variables—1, 3

Variable	Regression Coefficient	Standard Error Coefficient	Computed T
1	3.14 E−01	4.16 E−02	7.54 E+00
3	−4.31 E−01	1.96 E−01	−2.19 E+00

R-squared = 0.883.

2.8) Dependent Variable—7
Independent Variable—1

Variable	Regression Coefficient	Standard Error Coefficient	Computed T
1	3.57 E−01	4.16 E−02	8.58 E+00

R-squared = 0.840.

2.9) Dependent Variable—7
Independent Variable—3

Variable	Regression Coefficient	Standard Error Coefficient	Computed T
3	−1.12 E+00	3.88 E−01	−2.89 E+00

R-squared = 0.373.

2.10) **Dependent Variable—7**
Independent Variable—2

Variable	Regression Coefficient	Standard Error Coefficient	Computed T
2	1.37 E−01	1.02 E+00	1.34 E−01

R-squared = 0.001.

2.11) **Dependent Variable—8**
Independent Variables—1, 2, 3

Variable	Regression Coefficient	Standard Error Coefficient	Computed T
1	1.24 E−01	4.95 E−02	2.50 E+00
2	2.66 E−01	4.50 E−01	5.92 E−01
3	1.85 E+00	2.42 E−01	7.62 E+00

R-squared = 0.866.

2.12) **Dependent Variable—9**
Independent Variables—1, 2, 3

Variable	Regression Coefficient	Standard Error Coefficient	Computed T
1	1.39 E−01	1.89 E−02	7.36 E+00
2	−9.72 E−02	1.71 E−01	−5.67 E−01
3	−2.15 E−01	9.22 E−02	−2.33 E−00

R-squared = 0.902.

2.13) **Dependent Variable—1**
Independent Variables—4, 5

Variable	Regression Coefficient	Standard Error Coefficient	Computed T
4	−6.33 E−04	6.42 E−05	−9.85 E+00
5	−2.08 E+00	4.95 E−01	−4.20 E+00

R-squared = 0.901.

ACKNOWLEDGMENTS

The authors would like to acknowledge the generous support of the Association of American Railroads, the Processing Research Institute of Carnegie-Mellon University, and the National Science Foundation, who sponsored this research. The authors wish to thank D. H. Stone, of the Association of American Railroads Research Center, who served as technical liaison for the project, W. Server and D. Ireland of Dynatup for their valuable discussions concerning instrumented impact testing, and Professor J. R. Low, Jr. for valuable and fruitful discussions on the fracture of pearlite. Special thanks are due to Y. J. Park and G. K. Bouse, graduate students in the Department of Metallurgy and Materials Science at Carnegie-Mellon University, for experimental assistance, valuable discussions, and for permitting us to use some of their preliminary results. The findings presented herein were part of a final report submitted by J. M. Hyzak in partial fulfillment of the requirements for the degree of Master of Engineering at Carnegie-Mellon University.

REFERENCES

1. T. Gladman, I. McIvor, and F. Pickering: *J. Iron Steel Inst.*, 1972, vol. 210, p. 916.
2. M. Gensamer, E. B. Pearsall, W. S. Pellini, and J. R. Low, Jr.: *Trans. ASM*, 1942, vol. 30, p. 983.
3. T. Takahashi and M. Nagumo: *Trans. Jap. Inst. Metals*, 1970, vol. 11, p. 113.
4. J. Gross and D. Stout: *Weld. J.*, 1955, vol. 34, p. 117S.
5. G. Burns and C. Judge: *J. Iron Steel Inst.*, 1956, vol. 182, p. 292.
6. A. Turkalo: *Trans. TMS-AIME*, 1960, vol. 218, p. 24.
7. R. Grange: *Met. Trans.*, 1971, vol. 2, p. 65.
8. American Society for Testing Materials, 1974 Standard Designation E-112.
9. D. Brown and R. Ridley: *J. Iron Steel Inst.*, 1966, vol. 204, p. 812.
10. R. A. Wullaert: ASTM STP 466, p. 148, 1970.
11. G. E. Dieter: *Mechanical Metallurgy*, p. 370, McGraw-Hill, N.Y., 1961.
12. J. R. Vilella, G. E. Guellich, and E. C. Bain: *Trans. ASM*, 1936, vol. 24, p. 225.
13. B. Karlsson and G. Linden: *Mater. Sci. Eng.*, 1975, vol. 17, p. 153.
14. A. Rosenfield, E. Votava, and G. Hahn: *Trans. ASM*, 1968, vol. 61, p. 807.
15. A. Rosenfield, G. Hahn, and J. Embury: *Met. Trans.*, 1972, vol. 3, p. 2797.
16. U. Lindborg: *Trans. ASM*, 1968, vol. 61, p. 500.
17. C. S. Smith: *Trans. ASM*, 1953, vol. 45, p. 533.
18. R. J. Dippenaar and R. W. K. Honeycombe: *Proc. Roy. Soc., London*, 1973, vol. A333, p. 455.
19. Y. J. Park: Unpublished research, Department of Metallurgy and Materials Science, Carnegie-Mellon University, Pittsburgh, Pa., 1974.

APPENDIX REFERENCES

1a. W. Brown and J. Srawley: *Plane Strain Fracture Toughness Testing of High Strength Materials*, ASTM STP 410, 1966.
2a. F. J. Witt: *Equivalent Energy Procedures for Predicting Gross Plastic Fracture*, USAEC Report ORNL-TM3172, Oak Ridge National Laboratories, 1970.
3a. J. A. Begley and J. Landes: *Progress in Flaw Growth and Fracture Toughness Testing*, ASTM STP 536, p. 246, 1973.
4a. W. Server, D. Ireland, and R. Wullaert: *Strength and Toughness Evaluations from an Instrumented Impact Test*, Dynatup Report TR74-29R, 1974.